Conductance of Au/1,4-benzenedicarbothioamide/Au molecular junctions: a proposal for a potential linker

T. Sagisaka[a,1], S. Kurokawa[a], A. Sakai[a,*], K. -i. Yamashita[b], M. Taguchi[b], M. S. Asano[b], K. -i. Sugiura[b]

[a] *Department of Materials Science and Engineering, Kyoto University, Sakyo-ku, Kyoto 606-8501, Japan*
[b] *Department of Chemistry, Graduate School of Science and Engineering, Tokyo Metropolitan University, 1-1 Minami-Osawa, Hachioji-shi, Tokyo, 192-0397 Japan*

Abstract

We studied the conductance of Au/1,4-benzenedicarbothioamide (BDTA)/Au junctions at room temperature and measured a single-molecule conductance of BDTA. A carbothioamide (thioamide, $-CSNH_2$) group of this molecule consists of two potential linkers, thioketone and amine groups, and would thus be expected to show high conductance. The experimental single-molecule conductance of BDTA is $(0.8 - 1.0) \times 10^{-3} G_0$ which roughly compares with that of π-conjugated molecules. We consider that this relatively high conductance of Au/BDTA/Au is due to the homoconjugation of π-orbitals of benzene and sulfur while the amine group is likely to remain as a side group. We also observed that Au/BDTA/Au junctions can exist in multiple configurations of different conductances.

Keywords: molecular junctions, single-molecule conductance, Au/1,4-benzenedicarbothioamide/Au junctions, thioamide linker

*Corresponding author
Email address: sakai.akira.4z@kyoto-u.ac.jp (A. Sakai)
[1] Present address: SEIW, Kanuma-shi, Tochigi, 322-8585, Japan

1. Introduction

Single-molecule junctions have been a target of numerous theoretical and experimental studies in the past decades because of their primary importance in molecular electronic devices. [1, 2, 3, 4, 5, 6] Electron transport through molecules and molecule/electrode interfaces also involves a variety of unique conduction mechanisms, the studies of which have opened up a new field of molecular science. [7] In many single-molecule junctions, a bridging molecule consists of two parts, a core and a linker. The core part contributes to chemical activities of the junction and manifests designed functionalities. [8, 9, 10] On the other hand, the linker mechanically binds the molecule to the electrodes and also serves as an electronic interconnect between the electrodes and the core. Quite often, the linker controls the rate of electron transport across a junction and hence determines the junction conductance. [11] For obtaining highly conductive junctions, it is thus of crucial importance to design linkers that strongly couple to electrodes and accomplish high electron transmission. In previous experiments, various functional groups such as thiol (-SH), [12, 13, 14, 15, 16] amine, [14, 16, 17, 18] carboxyl, [14] and isocyano [15, 16, 19] groups have been employed as a potential linker which strongly interacts with Au electrodes. Among those, a thiol linker has been widely employed in many molecular junctions because of its stable metal-sulfur bonding. However, the reactive properties of thiol such as oxidative disulfide (-SS-) formation and nucleophilic addition/substitution reactions make the thiol linker unusable for designing further elaborated molecular devices. The authors focused in this work on carbothioamide (thioamide, $-\mathrm{CSNH_2}$) [20, 21, 22] as the best candidate for the linker. This functional group is stable under ambient condition and widely used as a *soft* ligand in coordination chemistry forming various complexes with *soft* acids including gold. As an archetypal molecular junction equipped with this new linker, we have designed 1,4-benzenedicarbothioamide (BDTA) where a benzene core connects to a pair of thioamide linkers each of which consists of two linkers, thioketone and amine groups, as illustrated in Fig. 1(a) (see also

Supporting Information 1 for 3D view of the molecule based on single crystal diffraction studies). If the thioketone and amine groups of thioamide cooperatively contribute for forming stable metal-molecule bonding and whereby enhancing electronic conduction, we can expect a high conductance for BDTA junctions. In this work, we present our experimental results on the conductance of Au/BDTA/Au single-molecule junctions measured at room temperature.

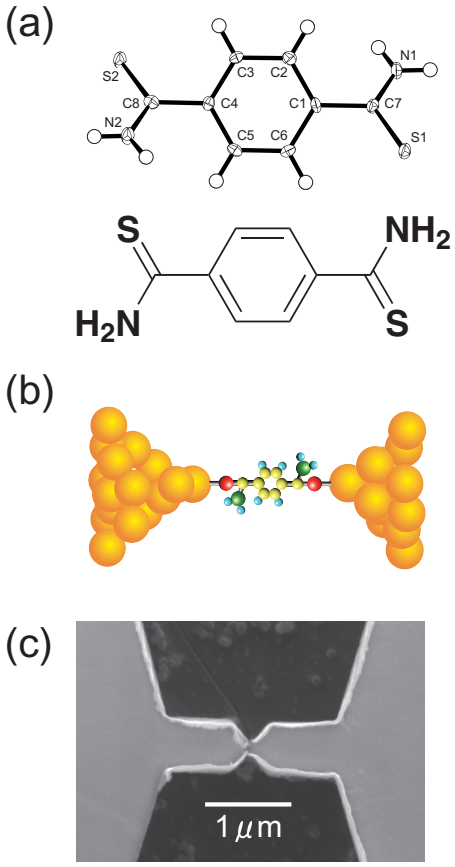

Figure 1: (a) Structure of BDTA determined by diffraction study and its schematic. The mean C=S and C-N distances are 1.680 Åand 1.318 Å, respectively. (b) Possible geometry of Au/BDTA/Au junction, and (c) SEM image of a microfabricated MCBJ used in our experiment.

2. Experimental methods

BDTA was prepared according to the literature. [23] The molecular structure determined by X-ray diffraction is shown in Fig. 1(a) (detailed structural information on BDTA can be found in Supporting Information 2). Compared to a benchmark BDT molecule, BDTA is slightly longer and has a larger sulfur-sulfur distance. It should also be emphasized that BDTA is not a planar molecule and the dihedral angle between benzene and thioamide planes is about 40°.

We employed mechanically controllable break junction (MCBJ) technique to produce single-molecule junctions. Our substrate is a 0.2 mm-thick stainless-steel sheet coated with a 25 μm-thick polyimide film for insulation. We deposited a 100nm-thick Cr/Au film on a substrate and microfabricated a bow-tie-shaped constriction shown in Fig. 1(c) by electron-beam lithography and lift-off. The designed constriction width is 200 nm. A pair of nanogapped electrodes is formed by bending the substrate and breaking the constriction. We used a linear translator and a piezo actuator for coarse and fine bending, respectively. The first junction break is made in a molecular solution to prevent contamination of freshly formed electrode surfaces. The molecular solution contains 0.3 mM BDTA in pure THF solvent (Wako Pure Chemical Industries, Ltd.). We repeatedly made open and close the junction under a constant bias of 100 mV and monitored a conductance trace, a temporal variation of the conductance, at each junction opening. Measurements were conducted at room temperature with junctions kept in the solution or placed in Ar atmosphere after pumping out the solution.

3. Results and discussion

When the solution contains no BDTA molecules, the conductance decreases exponentially with increasing the gap distance and exhibits a typical behavior of the tunneling conductance. After introducing BDTA molecules, the conductance trace often reveals plateau-like features as shown in Fig. 2. Such features can be often observed in conductance traces of various molecular junctions and

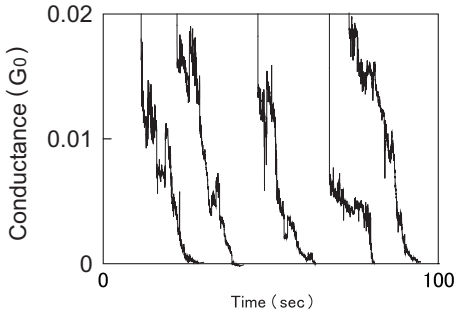

Figure 2: Examples of the conductance trace of the Au/BDTA/Au junction.

considered to signify a formation of molecular bridging between electrodes. The position of each plateau indicates the conductance of the corresponding molecular bridging. However, the plateau-like features are not reproducible and appear at different positions for different traces as seen in the figure. A standard remedy for treating such stochastic appearance of plateaus is to measure many conductance traces and put the data into a conductance histogram. Peaks in the histogram then indicate the conductances of some preferred junction geometries.

In this work, we carried out measurements in Ar on three different specimens and acquired 670 traces. To reduce a large background, we discarded featureless traces and adopted 163 traces. Similarly in solution, we obtained 1,363 on three specimens and selected 317 traces. The histograms constructed from these selected traces are shown Figs. 3(a) and 3(b) for measurements in Ar and in solution, respectively. In each panel, low-conductance and high-conductance histograms are displayed covering $G < 0.005G_0$ and $G < 0.02G_0$, respectively. Each histogram exhibits a couple of broad peaks superimposed on a smooth background. This background comes from the tunneling conduction and can be observed in a histogram obtained in the control experiment without BDTA, shown in the inset in Fig. 3(a). We found that this background varies with conductance G as $1/G$. Assuming this $1/G$-dependence for the background, we carried out the Gaussian peak fitting for the histograms shown in Figs. 3(a) and 3(b). In each figure, the red curve represents the $1/G$ background, the blue

peaks are Gaussian peaks (plus a constant) obtained from the fitting, and the green curve is the sum of all these contributions. Though peaks are broad and exhibit larger width at higher conductances, the green curve in each histogram well reproduces the observed intensity profile and the overall fitting appears satisfactory. We also note that the measurements in Ar and in solution make no significant differences on the peak positions.

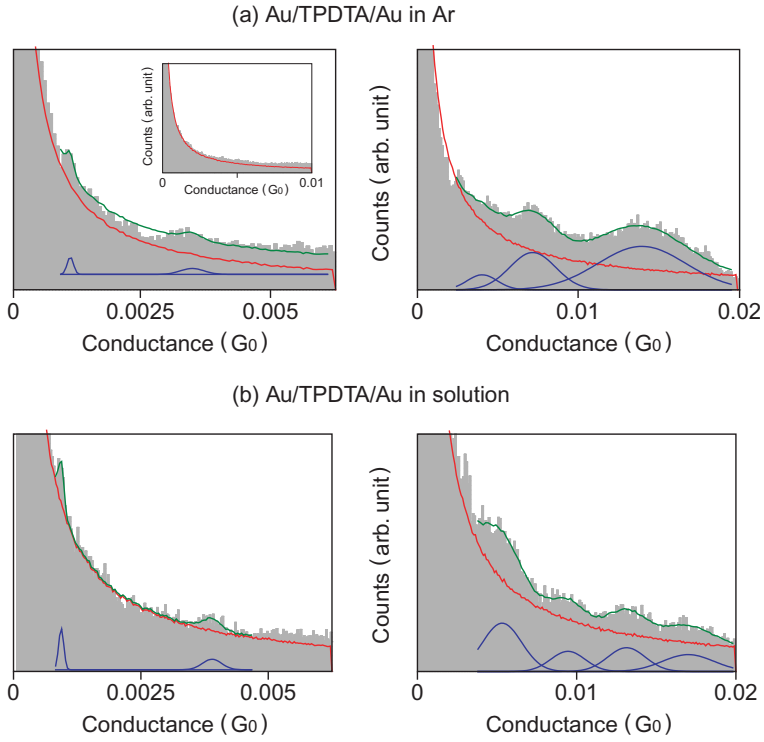

Figure 3: Conductance histograms of the Au/BDTA/Au junction measured in Ar (a) and in solution (b), respectively. Histograms in low- and high-conductance regimes are displayed separately. An inset in (a) shows a featureless histogram obtained in a control experiment without BDTA. In each histogram, the red curve represents the $1/G$ background, the blue peaks are Gaussian peaks obtained from the fitting, and the green curve is the sum of these peaks and the background. As seen in the inset, the smooth $1/G$ background well approximates the histogram of the control experiment.

We plot in Fig. 4 the positions of the conductance peaks. As seen in the figure, the conductance peak positions are not equidistant but nonlinearly increases with a peak index. The peaks cannot, therefore, be the result of multiple molecular bridging but likely to represent different geometries of Au/BDTA/Au

junctions. Possible origin of these peaks will be discussed later.

As mentioned before, we discarded featureless traces when constructing the histograms in Fig. 3. To examine the influence of this data selection on the conductance peaks, we built up for each measurement a conductance histogram using all traces acquired in that measurement. Though each histogram thus obtained shows not all but some of the observed peaks, eight histograms in total reproduce all peaks shown in Fig. 4. We also constructed another set of eight histograms from conductance traces measured at junction closing and found that these junction-closing histograms show all peaks in Fig. 4. From these results, we consider that the observed peaks are genuine conductance peaks of Au/BDTA/Au and unaffected by the data selection.

The first conductance peak in the histogram is customarily associated with a single-molecule bridging. Then, the result shown in Fig. 4 indicates that the single-molecule conductance of Au/BDTA/Au junction is $(0.8 - 1.0) \times 10^{-3} G_0$. This value can be compared with those of benzenedimethanethiol (BDMT) and benzenedicarbodithiol (BDCDT) molecules that have the same benzene core as BDTA but with different linker groups. The reported single-molecule conductance of these molecules, when bridging between Au electrodes, is $1 \times 10^{-4} G_0$ and $4.8 \times 10^{-3} G_0$ for BDMT [12] and BDCDT, [4, 24] respectively. Thus, the conductance of BDTA is 10 times higher than that of BDMT and approximately 20% of that of BDCDT. We also note that the conductance of BDTA is (10-30)% of that of shorter molecules such as BDT, 1,4-benzenediamine ($(6 - 7) \times 10^{-3} G_0$), [17] and 1,4-diisocyanobenzene ($3 \times 10^{-3} G_0$). [19] Among these molecules, latter three molecules have a conductive π-conjugated state that extends over the entire molecule and achieves high electron transmission. On the other hand, in BDTA, π-conjugated states exist at the benzene core but are terminated at two carbon atoms attached to the benzene core (*see* Supporting Information 2, Part-2, for Kohn-Sham frontier orbital diagrams of BDTA). The same disruption of π-conjugation also occurs for BDMT and BDCDT and explains the low conductance of BDMT. In the case of BDCDT, its high conductance would be the result of its two sulfur linkers. For BDTA, contrary to our initial ex-

pectation, not both of its thioketone and amine groups but only the thioketone group would serve as a linker to the Au electrode as will be mentioned later. BDTA is thus similar to BDTA for molecular conduction but still shows much higher conductance. As we have shown in Supporting Information 2, a BDTA molecule exhibits smaller HOMO-LUMO gap ($\Delta E = 3.51$ eV) than that of BDT ($\Delta E = 5.28$ eV). This gap narrowing is due to homoconjugation, a significant overlapping between π-orbitals of sulfur and benzene through space, though they are separated by a non-conjugating carbon atom. Presumably, the homoconjugated π-orbitals bypass the blocking carbon atoms and would provide a conductive channel for electronic transport across the molecule. After the sulfur atom makes a bond to the Au electrode, this homoconjugation might be more or less affected. It is, however, still likely that the sulfur-benzene homoconjugation survives in Au/BDTA/Au junctions and contributes to increasing their conductance.

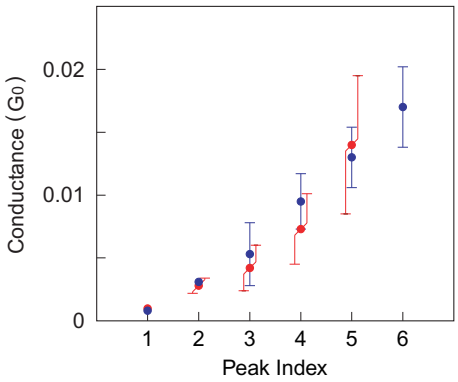

Figure 4: Positions of conductance peaks obtained from histograms measured in Ar (red dots) and in solution (blue dots), respectively.

Compared to the thioketone group, we consider that the amino group makes a secondary contribution to the conductance. Recent HREELS measurements [25] on SAMs of alkanethioamide molecules on Au(111) suggest that only the thiol group makes a strong bond to an Au substrate, while the amine group remains as a side group, as illustrated in Figs. 1(b). Electron transport would be mainly accomplished through the thioketone group with the help of the ho-

moconjugation between sulfur and benzene as mentioned above. It might be possible, however, that the amine group affects the conductance. As a side group, the amine group should be weakly coupled to the Au electrode and able to take various geometries. This configurational freedom of the amine group allows an Au/BDTA/Au junction to exist in a multiple of bridging configurations that are stable and show different conductances. These bridging configurations might correspond to the multiple peaks shown in Fig. 4, but proving this correspondence requires elaborate conductance calculations combined with geometry optimization for a molecule and electrode atoms. This should be our next step toward understanding the conductance characteristics of Au/BDTA/Au junctions. Our results on BDTA also suggest the importance of homoconjugation in the conduction of non-conjugated molecules. Also, as we noted before, the homoconjugation in BDTA tends to decrease its HOMO-LUMO gap. We hope that our work stimulates further exploration of the effects of homoconjugation on the molecule conductance and the intramolecular HOMO-LUMO gap.

4. Summary

We have experimentally studied the conductance of a double-linker molecule BDTA. Exploiting microfabricated MCBJs, we carried out measurements at room temperature in solution and in Ar atmosphere. The conductance histogram reveals multiple peaks, and the location of the first peak indicates $(0.8-1.0)\times10^{-3}G_0$ for the single-molecule conductance of BDTA. This conductance is still lower than but comparable with that of π-conjugated molecules. We consider that relatively high conductance of BDTA is due to the homoconjugation between the benzene core and sulfur atoms.

Acknowledgements

We thank Prof. M. Taniguchi (Osaka University), Prof. I. Kanno (Kobe University), Mr. E. Ohmura, and Mr. A. Wakasa for their support in making microfabricated MCBJs.

References

[1] J. M. Tour, Acc. Chem. Res. **33** (2000) 791.

[2] M. A. Reed, C. Zhou, C. J. Muller, T. P. Burgin, and J. M. Tour, Science **278** (1997) 252.

[3] X. Li, J. He, J. Hihath, B. Xu, S. M. Lindsay, and N. Tao, J. Am. Chem. Soc. **128** (2006) 2135.

[4] Y. Xing, T. -H. Park, R. Venkatramani, S. Keinan, D. N. Beratan, M. J. Therien and E. Borguet, J. Am. Chem. Soc. **132** (2010) 7946.

[5] G. Sedghi, K. Sawada, L. J. Esdaile, M. Hoffmann, H. L. Anderson, D. Bethell, W. Haiss, S. J. Higgins, R. J. Nichols, J. Am. Chem. Soc. **130** (2008) 8582.

[6] Q. Lu, K. Liu, H. Zhang, Z. Du, X. Wang, and F. Wang, ACS Nano **12** (2009) 3861.

[7] J. C. Cuevas and E. Scheer, *Molecular Electronics: An Introduction to Theory and Experiment* (World Scientific, Singapore 2010).

[8] I. Díez-Pérez, J. Hihath, Y. Lee, L. Yu, L. Adamska, M. A. Kozhushner, I. I. Oleynik, and N. Tao, Nature Chem. **1** (2009) 635.

[9] K. Matsuda, H. Yamaguchi, T. Sakano, M. Ikeda, N. Tanifuji, and M. Irie, J. Phys. Chem. C **112** (2008) 17005.

[10] Z. H. Xiong, D. Wu, Z. V. Vardeny, and J. Shi, Nature **427** (2004) 821.

[11] L. Venkataraman, Y. S. Park, A. C. Whalley, C. Nuckolls, M. S. Hybertsen. and M, L. Steigerwald, Nano Lett. **7** (2007) 502.

[12] X. Xiao, B. Xu, and N. J. Tao, Nano Lett. **4** (2004) 267.

[13] K. Stokbro, J. Taylor, M. Brandbyge, J. -L. Mozos, and Ordejón, Comput. Mat. Sci. **27** (2003) 151.

[14] F. Chen, X. Li, J. Hihath, Z. Huang, and N. Tao, J. Am. Chem. Soc. **128** (2006) 15874.

[15] C. -H. Ko, M. -J. Huang, M. -D. Fu, and C. -H. Chen, J. Am. Chem. Soc. **132** (2010) 756.

[16] W. Hong, D. Z. Manrique, P. Moreno-García, M. Gulcur, A. Mishchenko, C. J. Lambert, M. R. Bryce, and T. Wandlowski, J. Am. Chem. Soc. **134** (2012) 2292.

[17] L. Venkataraman, J. E. Klare, I. W. Tam, C. Nuckolls, M. S. Hybertsen, and M. L. Steigerwald, Nano Lett. **6** (2006) 458.

[18] J. Tobita, Y. Kato, and M. Fujihira, Ultramicroscopy **108** (2008) 1040.

[19] M. Kiguchi, S. Miura, K. Hara, M. Sawamura, and K. Murakoshi, Appl. Phys. Lett. **89** (2006) 213104.

[20] J. R. Dilworth and N. Wheatley, Coord. Chem. Rev. **199** (2000) 89.

[21] P. D. Akrivos, Coord. Chem. Rev. **213** (2001) 181.

[22] W. Zhang and M. Shi, Synlett, **1** (2007) 19.

[23] S. Dixon, and R. J. Whitby, Tetrahedron Lett. **47** (2006) 8147.

[24] A. V. Tivanski, Y. He, E. Borguet, H. Liu, G. C. Walker, and D. H. Waldeck, J. Phys. Chem. B **109** (2005) 5393.

[25] K. -i. Sugiura, *unpublished*.

Supporting Information 1

Molecular geometry of BDTA

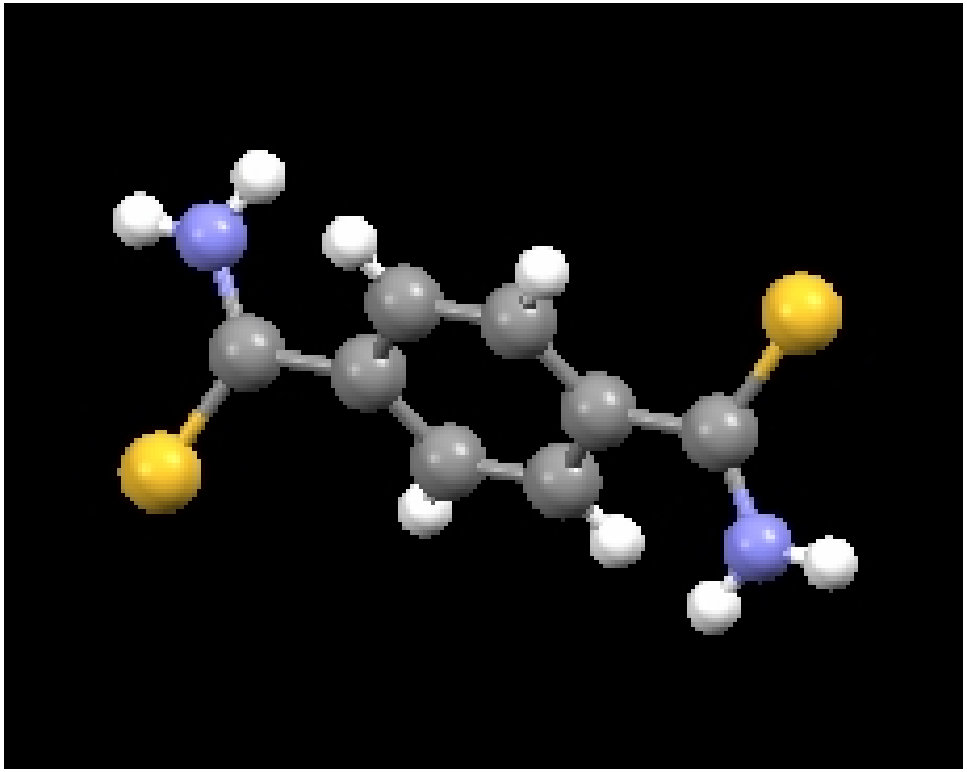

Supporting Information #2

Molecular Structures and Kohn–Sham Frontier Orbital Energies

Title: Conductance of Au/1,4-benzenedicarbothioamide /Au molecular junctions

Authors: Takami Sagisaka,[a] Shu Kurokawa,[a] Akira Sakai,[a]* Ken-ichi Yamashita,[b] Masateru Taguchi,[b] Motoko S. Asano,[b] and Ken-ichi Sugiura[b]

Organization: [a] Department of Materials Science and Engineering, Kyoto University, Sakyo-ku, Kyoto 606-8501 Japan

[b] Department of Chemistry, Graduate School of Science and Engineering, Tokyo Metropolitan University, 1-1 Minami-Ohsawa, Hachi-Oji, Tokyo 192-0397, Japan

Part-1
Molecular Structures of BDTA and BDT
Diffraction† and Theoretical†† Studies

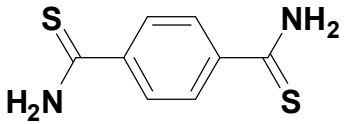

1,4-Benzenedicarbothioamide
(BDTA)

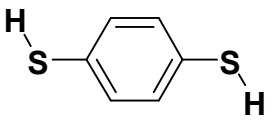

1,4-Benzenedithiol
(BDT)

† Diffraction Studies
The details of diffraction studies were summarized in Supporting Information #1

†† Our best knowledge is concerned, no single crystal diffraction study on BDT was reported.

††† Theoretical Studies
Program: Gaussian R-09W Ver.7 + Gauss View Ver.5
Method: B3LYP
Basis Set: 6-31G(d)

Important Bond Distances of BDTA (Å)

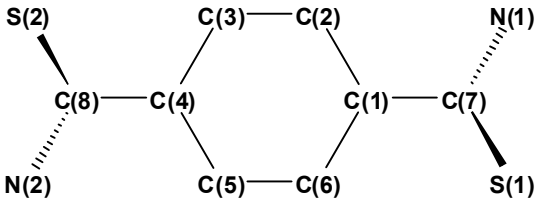

Bond	Diffraction Study		Theoretical Study
	Distance	Average	
S(1)-C(7)	1.683(3)	1.680	1.668
S(2)-C(8)	1.677(4)		
N(1)-C(7)	1.313(5)	1.318	1.353
N(2)-C(8)	1.322(5)		
C(1)-C(7)	1.484(5)	1.487	1.490
C(4)-C(8)	1.490(5)		
C(1)-C(2)	1.402(4)	1.398	1.407
C(4)-C(5)	1.393(4)		
C(2)-C(3)	1.380(5)	1.384	1.390
C(5)-C(6)	1.387(5)		
C(3)-C(4)	1.390(4)	1.393	1.402
C(6)-C(1)	1.395(4)		
S(1)-S(2)	8.016(2)		8.128

Important Bond and Dihedral† Angles of BDTA (degree)

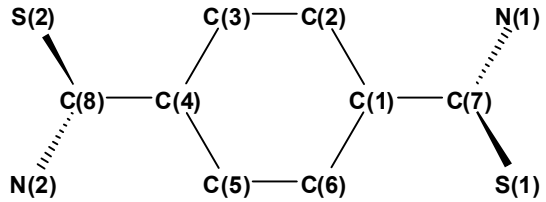

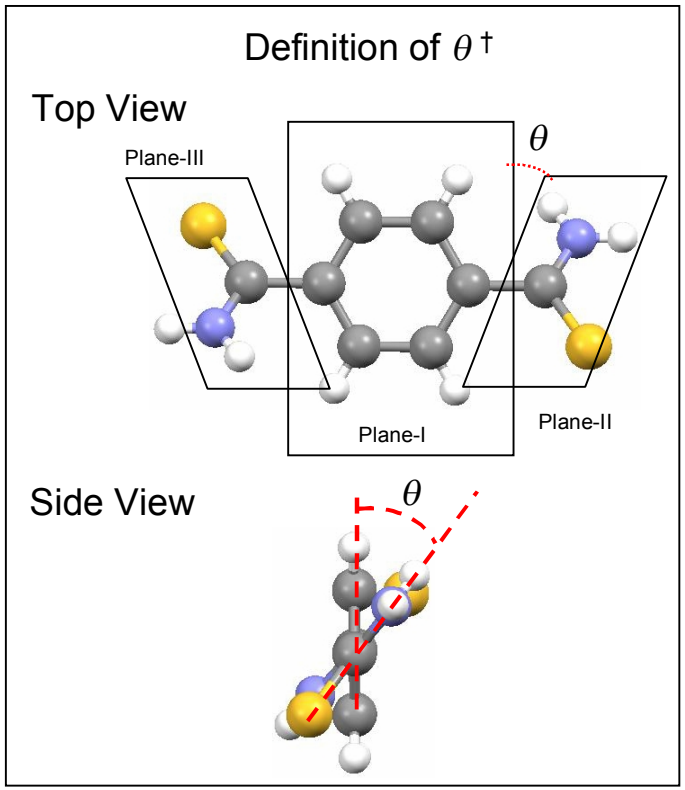

Angle	Diffraction Study		Theoretical Study
	Angle	Average	
∠C(1)-C(2)-C(3)	120.1(3)	120.2	120.9
∠C(4)-C(5)-C(6)	120.3(3)		
∠C(2)-C(3)-C(4)	120.7(3)	120.5	120.6
∠C(5)-C(6)-C(1)	120.2(3)		
∠C(3)-C(4)-C(5)	119.4(3)	119.3	118.5
∠C(6)-C(1)-C(2)	119.2(3)		
∠C(7)-C(1)-C(2)	120.4(3)	120.5	121.2
∠C(8)-C(4)-C(5)	120.5(3)		
∠C(7)-C(1)-C(6)	120.4(3)	120.3	120.3
∠C(8)-C(4)-C(3)	120.1(3)		
∠C(1)-C(7)-N(1)	117.5(3)	117.1	114.9
∠C(4)-C(8)-N(2)	116.6(3)		
∠C(1)-C(7)-S(1)	120.3(2)	120.5	123.3
∠C(4)-C(8)-S(2)	120.6(2)		
∠N(1)-C(7)-S(1)	122.3(3)	122.6	121.7
∠N(2)-C(8)-S(2)	122.8(3)		
∠Plane-I, Plane-II	37.37(8)	39.6	31.6
∠Plane-I, Plane-III	41.81(8)		

† The dihedral angles θ between benzene and thioacetamide were calculated by the root mean squared planes defined by C(1)-C(2)-C(3)-C(4)-C(5)-C(6) (Plane-I), N(1)-C(7)-S(1) (Plane-II), and N(2)-C(8)-S(2) (Plane-III). Calculations of θ were performed on Mercury Ver.3 (Cambridge Crystallographic Data Centre).

Important Bond Distances of BDT (Å)

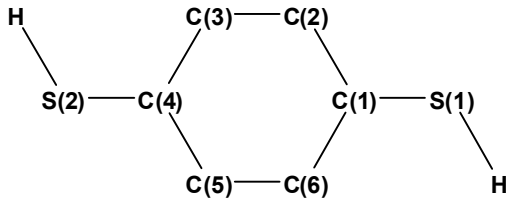

Bond	Theoretical Study
S(1)-C(1)	1.788
C(1)-C(2)	1.400
C(2)-C(3)	1.393
C(3)-C(4)	1.400
S(1)-S(2)	6.392

Part-2
Kohn–Sham Frontier Orbital Energies† of BDTA and BDT††

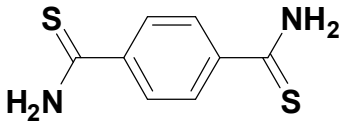

1,4-Benzenedicarbothioamide
(BDTA)

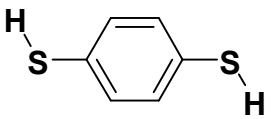

1,4-Benzenedithiol
(BDT)

† Theoretical Studies

Program:	Gaussian R-09W Ver.7 + Gauss View Ver.5
Method:	B3LYP
Basis Set:	6-31G(d)

†† The planer structure was obtained as the most stable structure for BDT.

Kohn–Sham Frontier Orbital Energies of BDTA and BDT

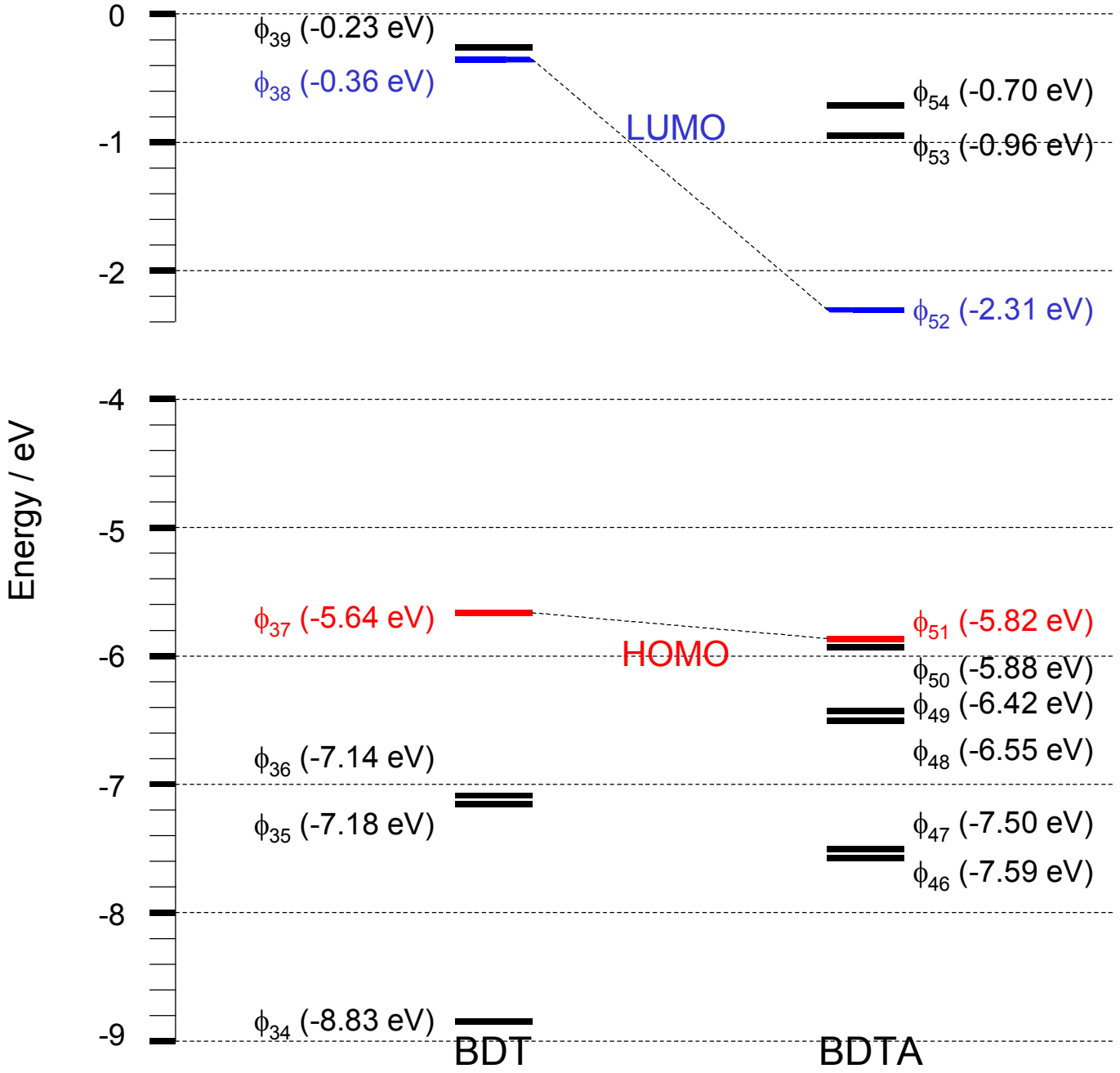

Kohn–Sham Frontier Orbitals of BDTA (1)

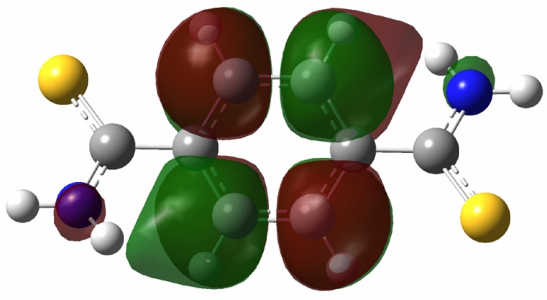

ϕ_{54}
-0.70 eV
LUMO+2

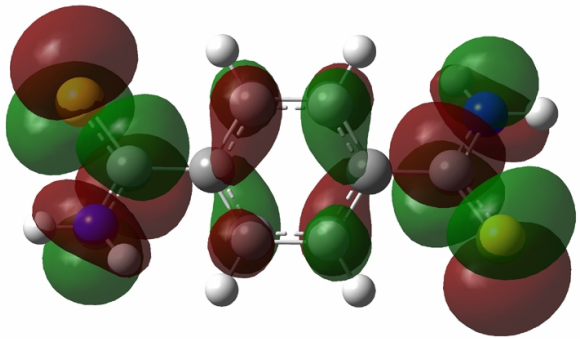

ϕ_{53}
-0.96 eV
LUMO+1

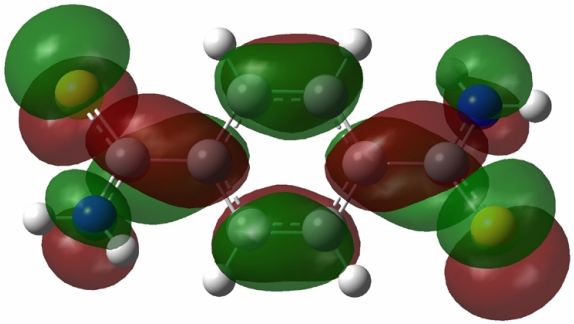

ϕ_{52}
-2.31 eV
LUMO

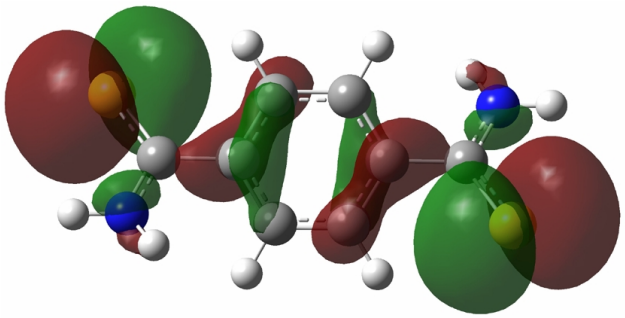

ϕ_{51}
-5.82 eV
HOMO

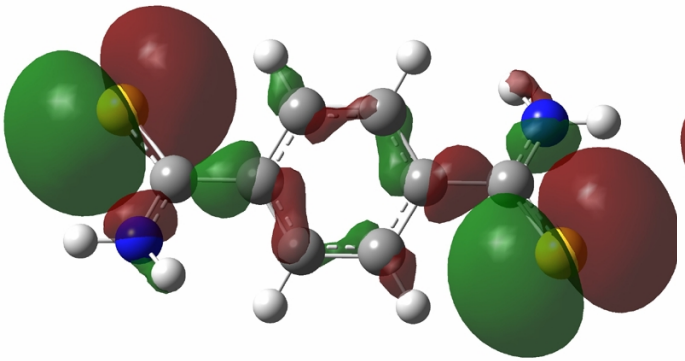

ϕ_{50}
-5.88 eV
HOMO-1

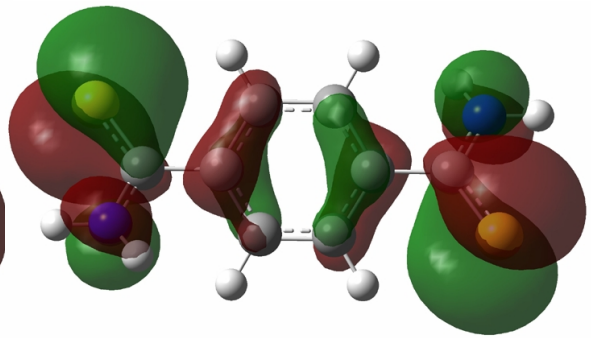

ϕ_{49}
-6.42 eV
HOMO-2

Kohn–Sham Frontier Orbitals of BDTA (2)

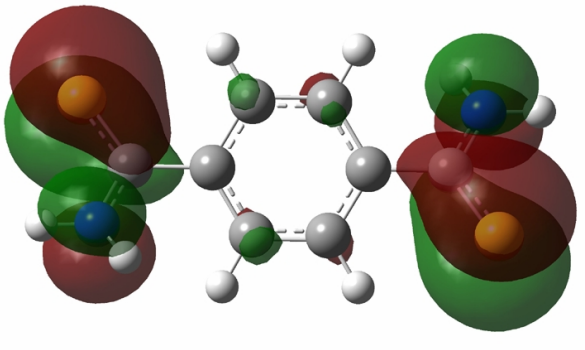

ϕ_{48}
-6.55 eV

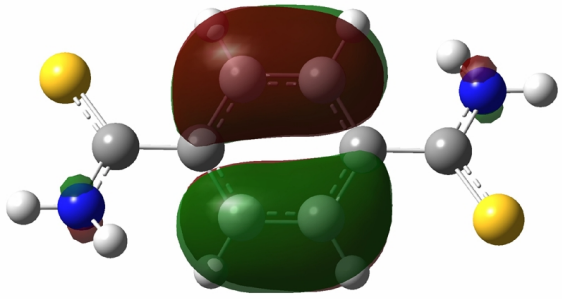

ϕ_{47}
-7.50 eV

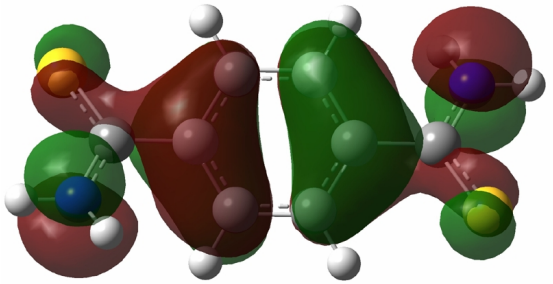

ϕ_{46}
-7.59 eV

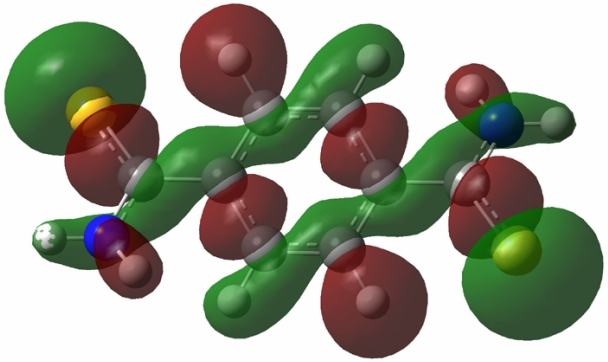

ϕ_{45}
-9.59 eV

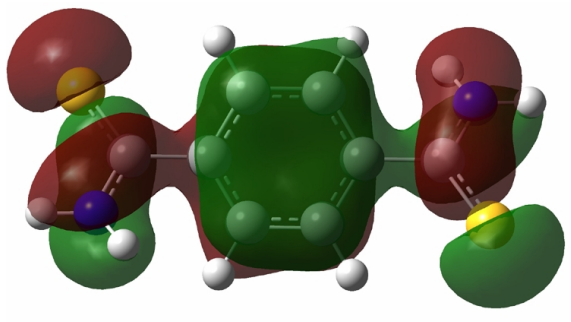

ϕ_{44}
-9.77 eV

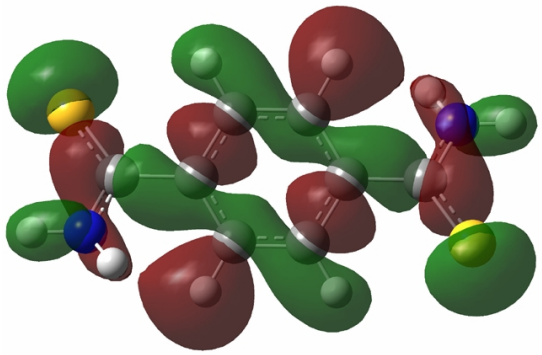

ϕ_{43}
-10.10 eV

Kohn–Sham Frontier Orbitals of BDT (1)

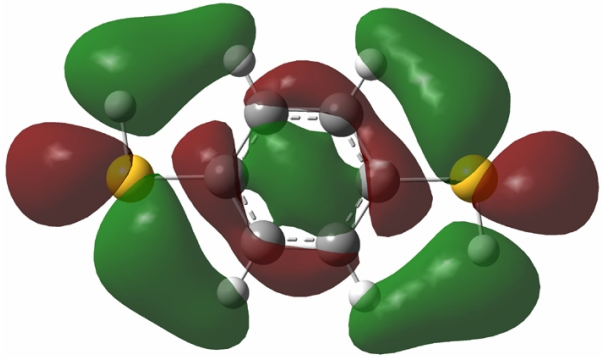

ϕ_{40}
+0.10 eV
LUMO+2

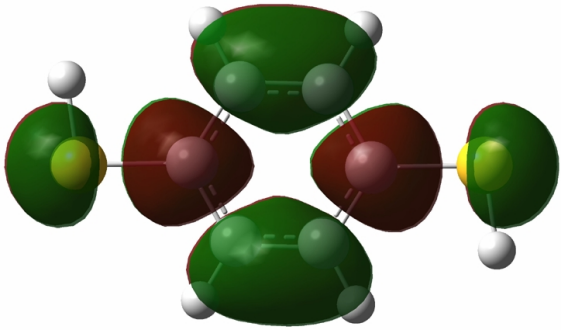

ϕ_{39}
-0.23 eV
LUMO+1

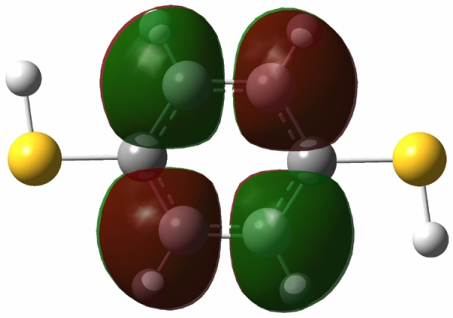

ϕ_{38}
-0.36 eV
LUMO

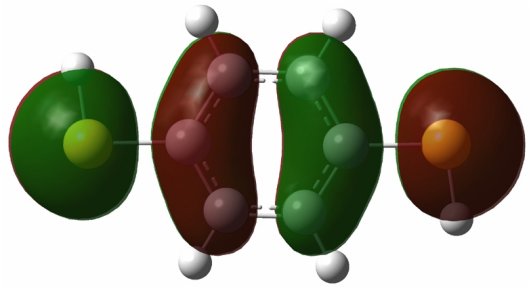

ϕ_{37}
-5.64 eV
HOMO

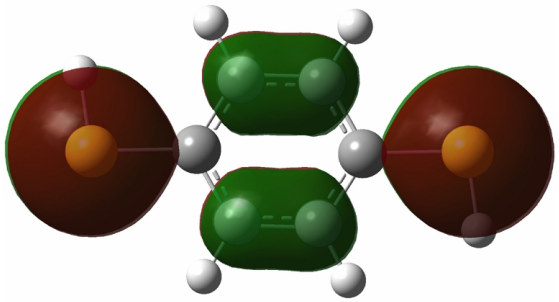

ϕ_{36}
-7.14 eV
HOMO-1

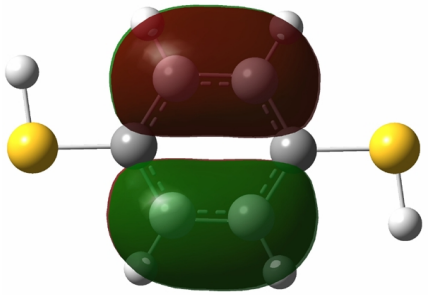

ϕ_{35}
-7.18 eV
HOMO-2

Kohn–Sham Frontier Orbitals of BDT (2)

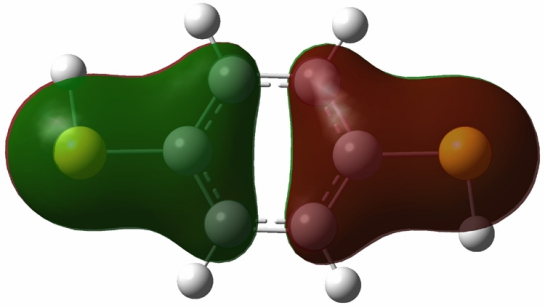

ϕ_{34}
-8.83 eV

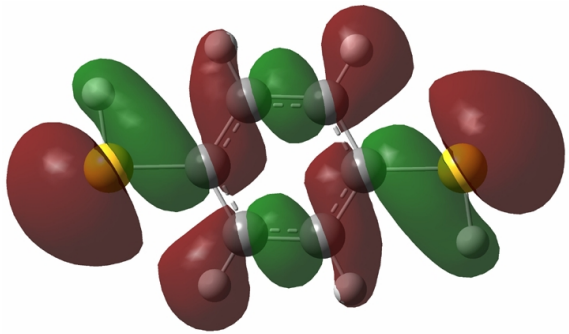

ϕ_{33}
-9.15 eV

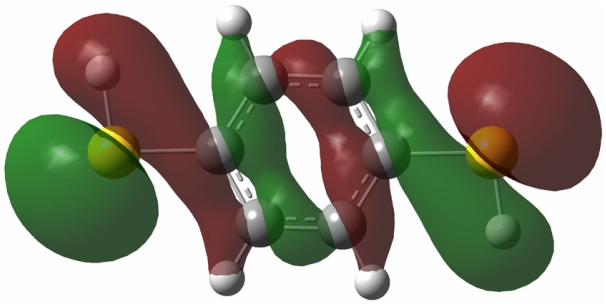

ϕ_{32}
-9.67 eV

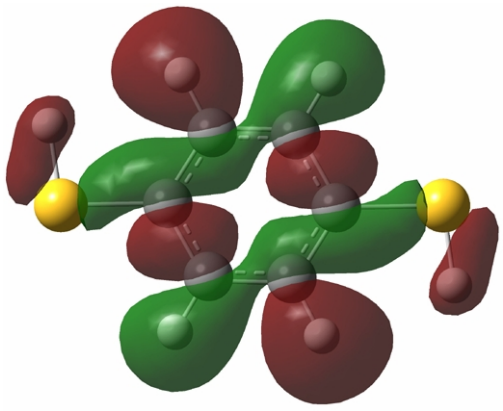

ϕ_{31}
-9.84 eV

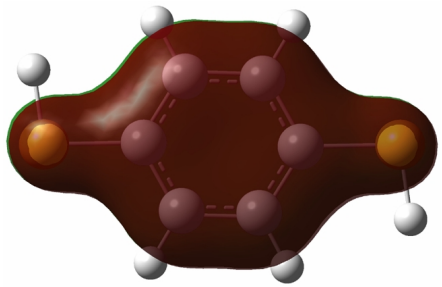

ϕ_{30}
-10.65 eV

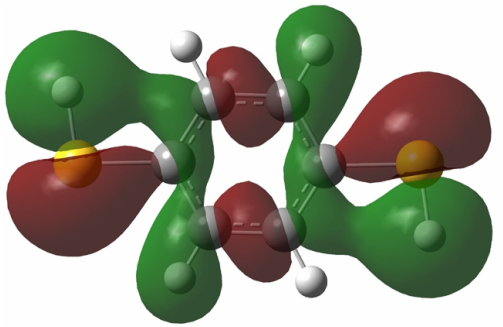

ϕ_{29}
-11.04 eV